Environmental risk of arsenic mobilization from disposed sand filter materials

Anh Van Le[a], *E. Marie Muehe*[b,c], *Soeren Drabesch*[a], *Juan Lezama Pacheco*[d], *Timm Bayer*[a], *Prachi Joshi*[a], *Andreas Kappler*[a, e], *Muammar Mansor*[a*],

[a]Geomicrobiology, Department of Geosciences, University of Tuebingen, 72076 Tuebingen, Germany [b]Plant Biogeochemistry, Department of Geosciences, University of Tuebingen, 72076 Tuebingen, Germany

[c]Plant Biogeochemistry, Department of Environmental Microbiology, Helmholtz Centre for Environmental Research - UFZ, 04318 Leipzig, Germany

[d]Department of Earth System Science, Stanford University, Stanford, California 94305, United States

[e]Cluster of Excellence: EXC 2124: Controlling Microbes to Fight Infection, University of Tuebingen, 72076 Tuebingen, Germany

*Corresponding author: Muammar Mansor, Geomicrobiology, Department of Geoscience University of Tuebingen, Schnarrenbergstrasse 94-96, D-72076 Tuebingen, Germany

Phone: +49 7071 - 29 78999, Email: muammar.muammar-bin-mansor@uni-tuebingen.de

For submission to Environmental Science and Technology

ABSTRACT

Arsenic (As)-bearing water treatment residuals (WTRs) from household sand filters is usually disposed on top of floodplain soils and may act as a secondary As contamination source. We hypothesized that open disposal of these filter-sand to soils will facilitate As release under reducing conditions. To quantify the mobilization risk of As, we incubated filter-sand, soil, and a mixture of filter-sand and soil in anoxic artificial rainwater and followed the dynamics of reactive Fe and As in aqueous, solid, and colloidal phases. Microbially-mediated Fe(III)/As(V) reduction led to the mobilization of 0.1-4% of total As into solution, with the highest As released from the mixture microcosms equaling 210 µg/L. Due to filter-sand and soil interaction, Moessbauer and X-ray absorption spectroscopies indicated that up to 10% Fe(III) and 32% As(V) was reduced in the mixture microcosm. Additionally, the mass concentration of colloidal Fe, and As analyzed by single-particle ICP-MS, decreased by 77-100% compared to the onset of reducing conditions, with the highest decrease observed in the mixture setups (>95%). Overall, our study suggests that (i) soil provides bioavailable components (e.g., organic matter) that promote As mobilization via microbial reduction of As-bearing Fe(III) (oxyhydr)oxides and (ii) As mobilization as colloids is important especially right after the onset of reducing conditions, but its importance decreases over time.

KEYWORDS: arsenic-bearing water treatment residuals, open disposal, disposed filter-sand, , microbial reduction, colloidal transport, arsenic remobilization.

SYNOPSIS: Filter-sand and soil interaction led to greater mobilization of dissolved As and lower mobilization of colloidal As in comparison to the absence of sand-soil interaction. **GRAPHICAL**

ABSTRACT

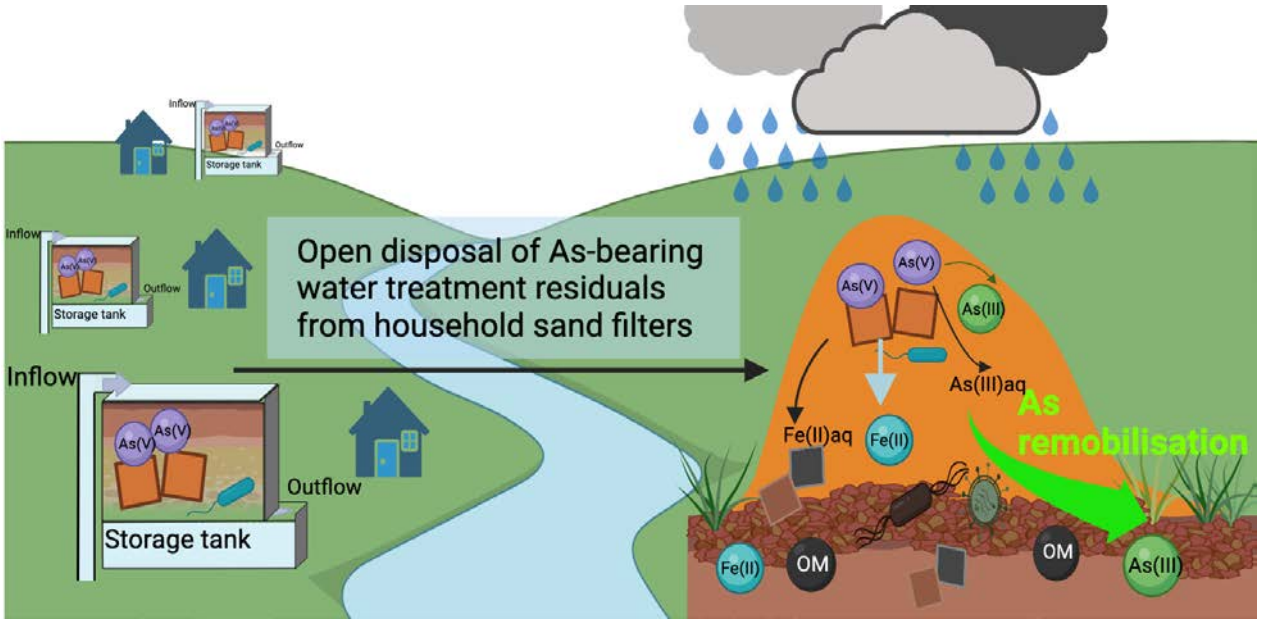
Open disposal of As-bearing water treatment residuals from household sand filters
Inflow
Outflow
Storage tank
As(V)
As(III)
As(III)aq
Fe(II)aq
Fe(II)
OM
As remobilisation

INTRODUCTION

Drinking water treatment facilities generate vast quantities of residuals that are enriched in contaminants(Ippolito et al., 2011; Turner et al., 2019). These water treatment residuals (WTRs) are commonly discharged in landfills in regions with sufficient space and resources(Clancy et al., 2013; Sullivan et al., 2010). However, in As-affected areas in rural South Asia, management of As-bearing WTRs is poor, leading to the open disposal of As-bearing WTRs to ponds, rivers, and soils without any site preparation(Genuchten et al., 2022; Koley, 2022). A challenge in the management of As-bearing WTRs is inadequate testing procedures that are not representative of actual conditions in the disposal sites, thus leading to over- or underprediction of As remobilization(Clancy et al., 2013). Common leach test, such as the toxicity characteristic leaching procedure (TCLP) have been shown to underpredict As mobilization from WTRs in landfills(Ghosh et al., 2004; Islam et al., 2011), since the test do not account for microbial activities that change over long periods and redox fluctuations (Clancy et al., 2013; Sullivan et al., 2010). A recent study(Genuchten et al., 2022) indicated that open disposal strategies especially pose the highest potential risk to environment and human health.

In the Red River delta in Vietnam, household sand filters are regularly used to remove toxic As from groundwater for drinking purposes. The groundwater is filtered through a reactive sand layer by gravity, in which Fe and As co-oxidize and precipitate on the sand matrix(Nitzsche et al., 2015; Van Le et al., 2022; Voegelin, Andreas; Kaegi, Ralf; Berg, Michael; Nitzsche, Katja Sonja; Kappler, Andreas; Lan, Vi Mai; Trang, Pham Thi Kim; Göttlicher, Jörg; Steininger, 2014). Eleven million people rely on household sand filters in Vietnam (data in 2007)(Berg et al., 2007; Winkel et al., 2011). With an average 3.5 people per (reported in 2009)(General Statistics Office of Vietnam, 2011), this means that around 3.1 million household with sand filters. The implication of this is that around 2.1×10^5 tons of sand filter residues is openly disposed to the environment every

6 months (assuming 0.47 m^2 surface area, 1470 kg/m^3 density, 35% porosity, 10 cm of sand layer disposed every 6 months)(Voegelin, Andreas; Kaegi, Ralf; Berg, Michael; Nitzsche, Katja Sonja; Kappler, Andreas; Lan, Vi Mai; Trang, Pham Thi Kim; Göttlicher, Jörg; Steininger, 2014). The As mobilization risk from these staggering amount of materials has yet to be investigated. Other As contaminated sources from mining waste were previously reported to cause pollution to soil and crops around the disposal area(Ha et al., 2019; Hoang et al., 2021).

The mobilization risk of As from filter-sand is susceptible to redox alteration. Under oxic conditions, arsenic primarily exists as oxidized As(V) adsorbed to Fe(III) (oxyhydr)oxides(Voegelin, Andreas; Kaegi, Ralf; Berg, Michael; Nitzsche, Katja Sonja; Kappler, Andreas; Lan, Vi Mai; Trang, Pham Thi Kim; Göttlicher, Jörg; Steininger, 2014). During the monsoon season, with frequent and heavy rainfall and potential flood events, the disposed filter-sand turns anoxic and reducing, leading to a high risk of As release to the porewater. The general accepted mechanisms of As mobilization are via microbial reduction of As-bearing Fe(III) (oxyhydr)oxides(Connolly et al., 2022; Stuckey et al., 2016), as well as the direct reduction of As(V) to As(III) by As-reducing bacteria (AsRB)(Oremland and Stolz, 2003). As(III) has a lower adsorption affinity to Fe(III) (oxyhydr)oxides than As(V), and is thus more amenable to mobilization(Dixit and Hering, 2003).

Open disposal of As-contaminated filter-sand material to the topsoil leads to mixing with complex soil matrix that contains diverse microbial communities, organic matter (OM), and minerals (e.g., Fe-Al-Mn (oxyhydr)oxides). The interaction between disposed filter-sand (enriched with As) and soil, therefore potentially plays a crucial but poorly understood role in the fate of As. Another factor to consider is whether disposed filter-sand is mobilized in the form of colloids, similar to the transport mechanism of other toxic contaminants in natural waters(Hassellov and von der Kammer,

2008). We define colloids as small particles subject to suspension and mobilization; this definition encompasses particles with size ranges that are beyond the traditionally considered 1-µm size cutoff(Noël et al., 2020). An increase of mobilized colloidal Fe(III) (oxyhydr)oxides can further facilitate As(V) transport(Montalvo et al., 2018; Yao et al., 2020). At the same time, colloidal Fe(III) (oxyhydr)oxides are known to be more susceptible to microbial reduction than larger mineral aggregates, therefore possibly promoting solubilization of As-bearing colloidal Fe(III) minerals(Fan et al., 2018; Ma et al., 2018; Mansor and Xu, 2020). Thus, it is crucial to also consider colloid-facilitated transport of As to fully evaluate the risk of As mobilization(Bauer and Blodau, 2009; Gomez-Gonzalez et al., 2016; Mansor et al., 2021).

In this study, we performed microcosm experiments in which As-bearing WTRs from filter-sand, soil, and a mixture of filter-sand and soil were incubated under reducing conditions over 130 days. We followed changes in reactive Fe(II), Fe minerals, As redox states and coordination environment in the solid phase, and the dynamics of dissolved and colloidal Fe and As over time. The results allowed us to assess the mobilization risk of As from open disposal of sand filter material

MATERIALS AND METHODS

Field site and sample collection.

We collected disposed filter-sand materials from several household filters in Tu Nhien village (20.848518 N; 105.919483 E), around 25 km Southeast of Hanoi, Vietnam, inside the meander of the Red River. Soil samples (top 20 cm) were collected from several gardens in the same village – we collected soils that were not in contact before with disposed filter material. Filter-sand and floodplain soils were collected in 5 independent replicates immediately cooled on ice during

transport, and stored at 4°C. In the laboratory, filter-sand or floodplain soils were used alone (100%) or mixed at a ratio of 1:1 before being used for incubation experiments.

Filter-sand and soil samples characterization.

The elemental composition (Fe, Al, P, As, Mn) of disposed filter-sand, floodplain soil, and the mixture of filter-sand and soil were analyzed by microwave digestion followed by inductively coupled plasma mass spectrometry analysis (ICP-MS) (Agilent 7900, Agilent Technologies). After drying in the oven (105°C), 0.5 grams of the sample was added to 12 ml of aqua-regia solution (9 ml of 37% HCl and 3 ml of 65% HNO_3) in Xpress Plus Teflon vessels. The samples were digested in the Microwave Accelerated Reaction System, MARS 6 (CEM, USA), with further details in SI section S1.

For total organic carbon (TOC) quantification, samples were dried at 60°C, grounded, and analyzed in triplicates with a soliTOC cube (Elementar Analysensysteme GmbH, Germany)

Microcosm experiments.

Microcosms were set up by adding 12.5 grams of disposed filter-sand, or soil, or pre-mixed 1:1 filter-sand and soil into 125 ml of sterile anoxic artificial rainwater (ARW; Table S1, section S2) within 250 ml serum bottles. Thus, the solid: liquid ratio is 1:10 in all bottles. The initial pH of all microcosms ranged from 6.8 to 7.3 (Table 1). Additionally, abiotic controls were amended with 160 mM sodium azide (NaN_3) to inhibit microbial respiration. All microcosms were prepared in triplicate in an anoxic glovebox (100% N_2, <30 ppm O_2, MBRAUN UNIlab). The microcosms were kept standing vertically at 28°C in the dark without shaking until analysis.

Solution chemistry analysis.

Immediately before sampling, the microcosms were homogenized by shaking. Aliquot suspensions (3 ml) were collected in two 2 ml Eppendorf tubes (1.5 ml in each) and centrifuged for 15 min at

12,100 g in the glovebox. The supernatants was filtered (0.22 µm cellulose filter, EMD Millipore) and diluted with 1% HNO_3 for quantification of dissolved Fe and As by ICP-MS. Sediment pellets remaining after centrifugation were either extracted with (a) 1 ml 0.5 M HCl for 2 hours (to quantify bioavailable/ poorly crystalline Fe) or (b) 1 ml 6 M HCl for 24 hours (to quantify crystalline Fe)(Schaedler et al., 2018). Afterwards, all samples were centrifuged at 15 min at 12100g, and 100 µl of the supernatant was collected and diluted 10-folds with 1 M HCl before analysis. HCl-extractable Fe(II) and Fe(total) were quantified spectrophotometrically using the ferrozine assay(Stookey, 1970; Viollier et al., 2000).

Iron mineral analysis using Moessbauer spectroscopy.

Moessbauer spectroscopy was used to identify Fe minerals. Pre-incubation samples were loaded as dried powders into 1 cm^2 Plexiglas holders. Solids from the microcosms collected by filtration (0.45 µm nitrocellulose filter, Millipore) were fixed between two pieces of Kapton tape in the glovebox and kept frozen and anoxically at -20°C in a sealed bottle until measurement. Spectra were collected at 77 K and 5 K using a constant acceleration drive system (WissEL) in transmission mode with a ^{57}Co/Rh source. Analyses were carried out using Recoil (University of Ottawa) and the Voigt Based Fitting (VBF) routine(Lagarec and Rancourt, 1997).

X-ray absorption spectroscopy (XAS).

To identity As redox states and binding environments, samples were collected prior to incubation and from the microcosms, then freeze-dried, ground, and stored anoxically until measurement.

Reference model compounds were synthesized in an anoxic glovebox by adsorbing arsenate ($Na_2HAsO_4x7H_2O$, Sigma-Aldrich) and arsenite ($AsNaO_2$, Sigma-Aldrich) onto ~30 mg of freshly prepared 500 mM ferrihydrite(Muehe et al., 2013) in a molar ratio of 30:1 for 10 hours with gentle overhead-mixing. Model compounds were washed twice in anoxic MQ water, freeze-dried, ground and diluted with approximately 26 mg of boron nitride and stored anoxically until measurement.

Samples and standards were placed in aluminum sample holders (window 3 mm by 13 mm) and sealed with 0.5 mil Kapton tape from both sides. Arsenic K-edge extended X-ray absorption fine structure (EXAFS) data were obtained at beamline 7-3 at Stanford Synchrotron Radiation Lightsource (SSRL), Menlo Park, USA. Spectra were collected in fluorescence detection mode using a 30-element germanium detector array, using a reference gold foil in transmission detection mode and calibrating to 11919 eV. More details on beamline settings are given in SI section S3. Data was deadtime-corrected and averaged with Sixpack(Webb, 2005) and repetitive scans aligned, merged, truncated, deglitched, normalized to an edge step of one, and background-subtracted in Athena(Ravel and Newville, 2005). To verify data, XANES (extracted from EXAFS) and EXAFS were analyzed for As speciation differences. Principle components (PCA) and target transforms were analyzed for merged scans, followed by least-square fitting by linear combination (LCF) of synthesized model compound spectra(Muehe et al., 2016). EXAFS were analyzed to a k of 12. The LCF components are estimated to be accurate at 10% and the detection limit of contributing components is set to 10%(Cancès et al., 2005; O'Day et al., 2004). Shell-by-shell fitting was performed to support LCF fits, given in SI section S3.

Quantification of Fe and As in colloidal fraction.

Microcosms were shaken, and large particles were allowed to settle for 24 hours while standing in the glove box. Afterward, about 0.1 ml of suspension was carefully sampled directly from the top and stored anoxically at 4°C. The suspensions were diluted 1000-fold in anoxic H_2O in a Falcon tube in the glove box and taken out right before the analysis. All samples were analyzed in time-resolved analysis mode on an Agilent 7900 ICP-MS instrument(Mansor et al., 2021). More details are provided in SI section S4.

RESULTS AND DISCUSSION

Characterization of disposed filter-sand and floodplain soil prior to incubation experiments. Microwave digestion and TOC analyses were performed to quantify elemental (Fe, Al, P, As, Mn) and organic carbon contents. The samples contained 50-100 g/kg of Fe, 22-80 g/kg of Al, 1-5 g/kg of P, 29-1440 mg/kg of As, 540-1166 mg/kg of Mn, and 2-12 g/kg of TOC (Table 1). The filter-sand material was enriched in Fe, P, and As relative to the soil, with an enrichment factor of approximately 2, 5, and 50, respectively. The soil was enriched in Al, Mn, and organic carbon, with an approximate enrichment factor of 4, 2, and 6, respectively. Aqua regia extraction followed by microwave digestion most likely underestimated soil's total Fe and Al content due to poor extractability of Fe phyllosilicates(Raiswell et al., 1994). In contrast, Fe in disposed filter-sand material primarily exists as short-range ordered (SRO) Fe(III) (oxyhydr)oxides(Nitzsche et al., 2015; Voegelin, Andreas; Kaegi, Ralf; Berg, Michael; Nitzsche, Katja Sonja; Kappler, Andreas; Lan, Vi Mai; Trang, Pham Thi Kim; Göttlicher, Jörg; Steininger, 2014) that are easily extractable with aqua regia.

Table 1. Elemental compositions of floodplain soil, disposed filter-sand material, and the mixture of filter-sand and soil prior to incubation. All samples were analyzed in triplicates.

	Floodplain soil	Disposed filter-sand material	Mixture of filter-sand and soil
Fe (g/kg)	50±4	97±6	76±8
Al (g/kg)	79±6	22±2	55±6
P (g/kg)	1±0.1	5±0.5	3±0.3
As (mg/kg)	29±3	1441±81	725±64
Mn (mg/kg)	1166±92	539±52	911±153
Fe/Mn ratio	42.5±0.1	182.4±28.3	84.3±6.3
Fe/As ratio	1723±39	67.5±0.6	105±3
TOC (g/kg)	11.7±0.4	3.2±0.2	7.2±0.2
Initial pH*	6.8	7.3	7.2

(*) Initial pH values of the microcosms

Dynamics of reactive Fe and As in floodplain soil and disposed filter-sand microcosms.

As- and Fe-rich sand filter materials are usually disposed onto the floodplain soil or along the riverbank. To evaluate the potential for As mobilization from the filter-sand after disposal, we first incubated filter-sand and soil samples separately with ARW under reducing conditions. Within 130 days of incubation, the color changed from orange/gray to a darker black in the biotic microcosms, indicative of Fe(III) reduction (Figure S1). The highest Fe(III) reduction took place in the soil microcosms, in which 0.5 M HCl-extractable Fe(II) increased from 0.008 to 4.6 g/kg sediment (Figure 1A). This equals to near-complete Fe(III) reduction from the 0.5 M HCl-extractable fraction (93±8%) (Figure S2A). In comparison, microcosms with filter-sand only displayed a limited extent of Fe(III) reduction, in which the 0.5 M HCl-extractable Fe(II) increased from 0.15 to 1.1 g/kg sediment (Figure 1A). This equals a reduction of only 6±1% of the poorly crystalline Fe pool (Figure S2A). Similar trends were observed in the 6 M-extractable Fe(II) and Fe(II)/Fe(total) ratios (Figure S2, S3 respectively), albeit with a lower magnitude of changes compared to the 0.5 M HCl-extractable fractions.

Dissolved total Fe was detected in small amounts in all microcosms; it increased from 2 to 4.2 mg/L in filter-sand microcosms. In contrast, the concentration remained around 0.7-0.9 mg/L in soil microcosms throughout the incubation (Figure 1B). Interestingly, even though total As in the soil was lower relative to the disposed filter-sand, we detected the constant release of As from soil to the aqueous phase from 3 to 115 µg/L over 130 days (Figure 1C). In comparison, dissolved As in filter-sand microcosms increased sharply during the first 40 days to around 150 µg/L, which then leveled off until the end of the experiment (Figure 1C). Abiotic controls for both microcosms showed low levels of Fe(III) reduction and As mobilization, possibly due to abiotic processes or incomplete inhibition of microbial activity by NaN_3(Bore et al., 2017) . 0.5 M HCl-extractable

Fe(II) and dissolved As were <0.5 g/kg and <60 μg/L, respectively, which were lower than the values observed in the experimental setups without microbial inhibition (Figure 1C).

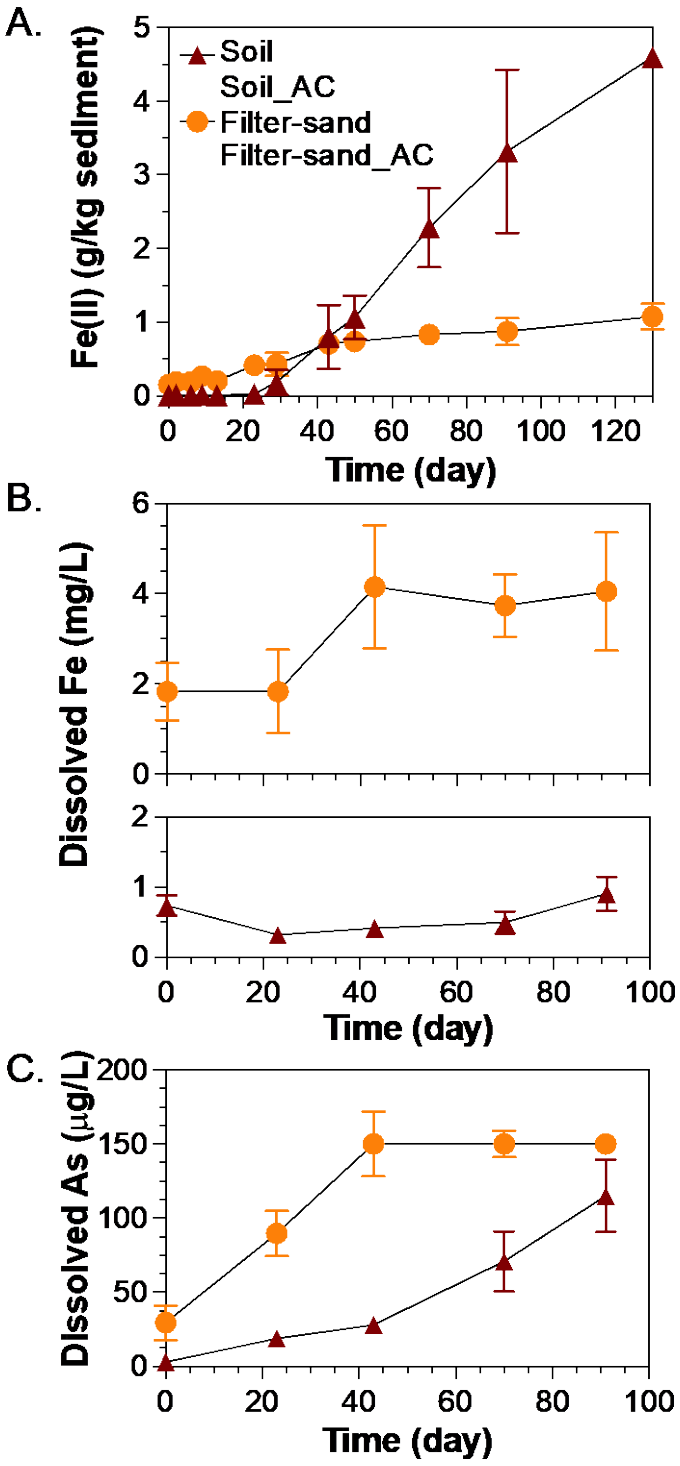

Figure 1. Changes in the concentration of 0.5 M HCl-extractable Fe(II) (A), dissolved Fe (B), and dissolved As (C) in floodplain soil, disposed filter-sand and their abiotic control (AC) microcosms. All samples were analyzed in triplicate, and error bars indicate standard deviation.

Dynamics of reactive Fe and As in the microcosm containing the mixture of filter-sand and soil.

We hypothesized that when disposed filter-sand is mixed with soil, the microbial community and/or organic matter from the soil matrix may promote As mobilization from the disposed filter-sand by stimulating microbial Fe(III) and As(V) reduction. Therefore, we followed changes of reactive Fe and As in the mixture of filter-sand and soil microcosms (termed "sand-soil interaction") and compared them to a "no-interaction" scenario. The values for the "no interaction" scenario were calculated by averaging the data obtained in soil-only and filter-sand only microcosms as a method of applying mass correction. This scenario, therefore, represents a hypothetical case that accounts for the mass of Fe and As in both soil and filter-sand and implicitly assumes the soil matrix plays no role in promoting or inhibiting Fe and As reduction.

By comparing the experimental sand-soil interaction case with the hypothetical "no interaction" case, we were able to clearly observe a promotive effect of sand-soil interaction to Fe(III) and As(V) reduction, which overall led to about twice more As being mobilized compared to "no interaction". The content of 0.5 M HCl-extractable Fe(II) increased significantly in the mixture of filter-sand and soil from 0.07 to 3.5 g/kg, which is 1.2 times higher than the "no interaction" case (Figure 2A). Similar trends were observed in the 6 M HCl-extractable Fe(II) and Fe(II)/Fe(total) ratios (figure S2, S3), albeit with a lower magnitude of changes compared to the 0.5 M HCl-extractable fractions.

The dissolved Fe concentration of the mixture microcosm was slightly lower than in the "no interaction" case. Dissolved Fe in the mixture of filter-sand and soil microcosms and abiotic control

252 at day 0 (immediately after setup of the microcosm) was higher than on other days. – We consider
253 this to be an outlier, possibly due to short-term mixing effects between the soil and filter-sand
254 materials. Disregarding these data points, dissolved Fe gradually increased from 0.7 mg/L on day
255 23 to 2.1 mg/L, but remained lower than the “no interaction” case throughout the incubation period
256 (Figure 2B).
257 Lastly, dissolved As showed a marked increase in the mixture setup (up to 210 µg/L) relative to
258 abiotic controls (maximum 90 µg/L) and the “no interaction” scenario (maximum 120 µg/L)
259 (Figure 2C). It means that As mobilization was promoted 1.8 times higher due to the sand-soil
260 interaction than the “no-interaction” case. Abiotic controls for the mixture microcosms showed
261 lower levels of Fe(III) reduction and As mobilization overall (Figure 2).
262

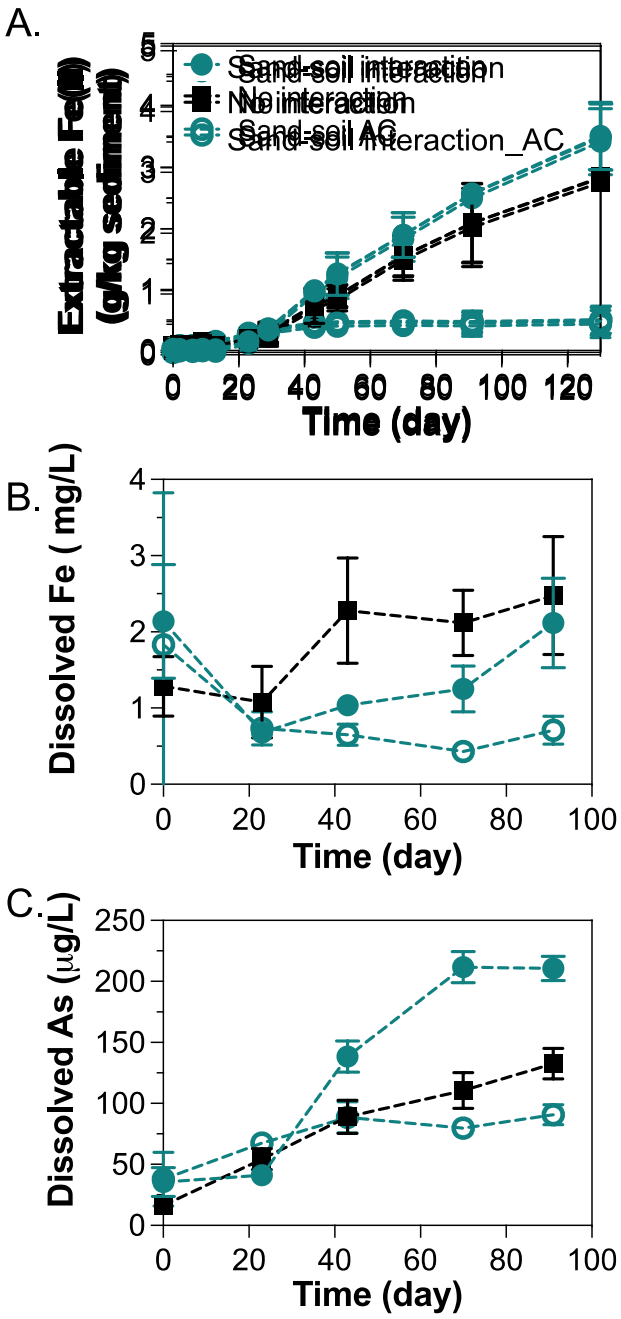

263

264 **Figure 2.** Comparison of Fe and As dynamics in the presence or absence of sand-soil interactions.
265 Changes of poorly crystalline Fe (0.5M HCl-extractable Fe), dissolved Fe and As of the sand-soil
266 interaction (mixture of filter-sand and soil) microcosms and their abiotic control (AC) microcosms
267 are shown in figure A, B, C respectively. The data is compared with corresponding value in the no-
268 interaction case. The no-interaction value is calculated with values obtained from soil only and

filter-sand only microcosms, assuming 1:1 mixture and no promotion or inhibition effects. All samples were analyzed in triplicate, and error bars indicate standard deviation.

Transformation of Fe minerals in the microcosms.

Changes in Fe mineralogy can affect the fate of As and were therefore followed by Moessbauer spectroscopy. Fitting results and Moessbauer spectra collected at 5 K and 77 K are shown in Table S2 and Figures S5-S7, respectively. The disposed filter-sand material prior to incubation consisted of 100% short-range-order (SRO) Fe(III) (oxyhydr)oxides (Figure 3A, Table S2), consistent with previous studies on sand filters(Nitzsche et al., 2015; Voegelin, Andreas; Kaegi, Ralf; Berg, Michael; Nitzsche, Katja Sonja; Kappler, Andreas; Lan, Vi Mai; Trang, Pham Thi Kim; Göttlicher, Jörg; Steininger, 2014). After 100 days of incubation, there was up to 14% of Fe(II) in the filter-sand matrix (Figure 3A), equaling a Fe(II)/Fe(III) ratio of 0.17 (Figure 3B), indicative of microbial Fe(III) reduction. In comparison, the soil initially contained a mixture of goethite (50%), low amounts of hematite (11%), Fe(III) phyllosilicates (25%), and Fe(II) (14%) (Figure 3A). The Fe(II) in the pre-incubation soil was likely in the form of phyllosilicates and not adsorbed Fe(II), as the soil had been sampled under oxic conditions. We observed a ~6.3% increase in Fe(II) after 100 days in the soil incubations, equaling a Fe(II)/Fe(III) ratio of 0.25 (Figure 3B). Note that the increased Fe(II) observed based on spectra collected at 5K may be slightly underestimated as the Fe(II) doublet can partially split at lower temperatures(Notini et al., 2018). Based on the spectra collected at 77K, the Fe(II) increased by 11% (Table S2). The mixture of filter-sand and soil microcosm showed Fe mineral distributions that reflect the end-member sand and soil, with detectable levels of goethite, SRO Fe(III) (oxyhydr)oxides, and Fe(II) and Fe(III) phyllosilicates. We observed an increase of around 3.4% Fe(II) in the mixture setup after 100 days (Figure 3) based

on the Mössbauer spectra at 5K and 10% based on spectra collected at 77K. We did not observe the formation of distinct Fe(II)-containing minerals such as magnetite or siderite.

In summary, we confirmed Fe(III) reduction in all microcosms. The filter-sand microcosm exhibited the highest relative increase in solid-phase Fe(II) over 100 days of incubation. This is because filter-sand material consisted of nearly 100% (SRO) Fe(III) (oxyhydr)oxides in the form of two-line ferrihydrite(Voegelin, Andreas; Kaegi, Ralf; Berg, Michael; Nitzsche, Katja Sonja; Kappler, Andreas; Lan, Vi Mai; Trang, Pham Thi Kim; Göttlicher, Jörg; Steininger, 2014), which is more thermodynamically available for microbial reduction than hematite and goethite(Kappler et al., 2021) found in soils.

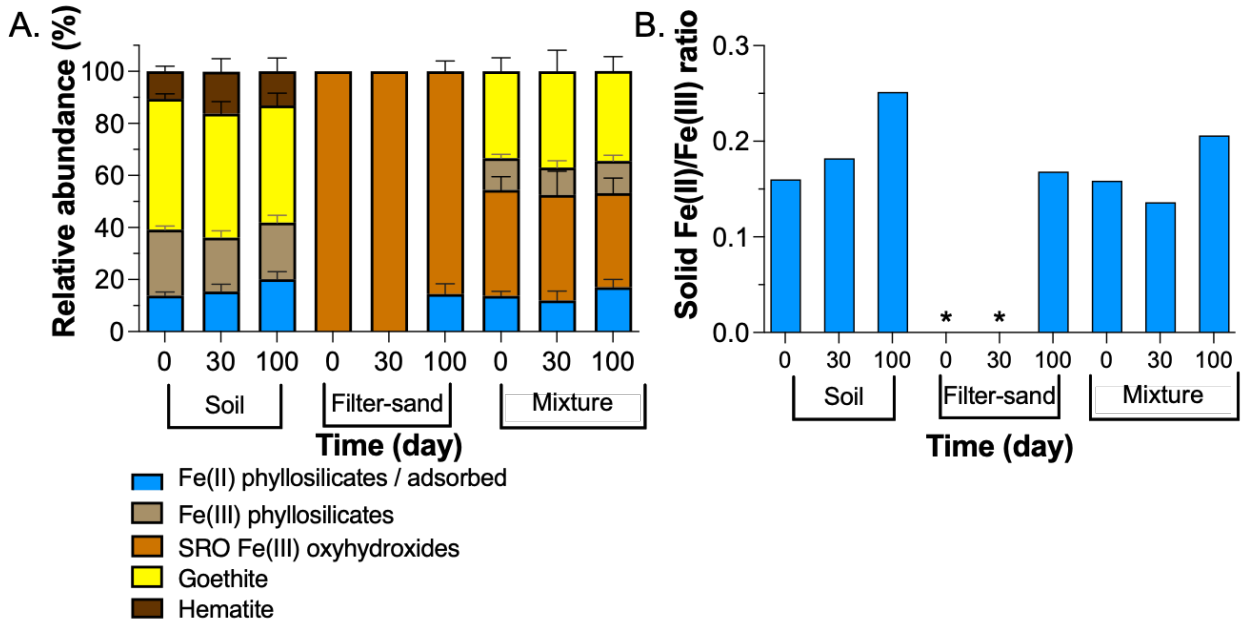

Figure 3. Fe mineralogy based on Moessbauer spectroscopy. Changes of relative abundance of Fe minerals, measured temperature at 5 K (A) and ratios difference of Fe(II)/Fe(III) phases (B) over time in 3 different microcosms (soil, filter-sand, and the mixture of filter-sand and soil). (*) No Fe(II) detected in sand microcosms at days 0 and 30.

Changes in solid phase As redox state and implications for As binding environment in the microcosms.

To determine changes in As redox states in the solid matrix, samples were analyzed at days 0, 30, and 84 by XANES and EXAFS at the As K-edge using a linear combination fitting (LCF) approach (Figures 4, S8, S9). XANES and EXAFS As speciation analyses showed comparable trends with minor differences in percentage contributions (Table S3). Arsenic redox distribution indicated that the disposed filter-sand and soil samples initially contained up to 90% As(V) and less than 10% As (III) (Figure 4A). After incubation, the As(III) contribution in sand microcosms increased by 23.6% of total As (Figure 4A). In the mixtures of filter-sand and soil, As(III) was increased by 32% of the total As pool (Figure 4A), corresponding to an increase of As(III) from 41.3 to 273 mg/kg (Figure 4B).

Analysis of As EXAFS data suggested As-Fe complex in all microcosms (at a distance of 2.88Å radial structure function equal to 3.3Å in real distances) (Figure 4C), corresponding to As-Fe inner-sphere complexes dominated by a bidentate-mononuclear edge-sharing (^{2}E) formation on the surface of Fe(III) (oxyhydr)oxides(Fendorf et al., 1997; Ona-Nguema et al., 2005). This type of complex might result from As-O-O-As multiple scattering(Manning et al., 1998; Ona-Nguema et al., 2005; Sherman and Randall, 2003). Overall, As K-edge EXAFS to the k of 12 were not able to resolve outer-sphere As binding beyond 3.5Å, which were more typically found above 5Å(Catalano et al., 2008). Shell-by-shell fits did not show any clear trend for As coordination differences between sand, soil and sand-soil mixture (SI Table S4). On a more descriptive note, in the mixture samples at day 30 and 84 and not in the filter-sand only or soil only microcosms, a shift from 2.88Å (= 3.3Å in real distances) to lower Å was observed compared to day 0. This shift caused the 2.88Å peak to be more diffuse suggesting that an outer-sphere As binding contribution possibly

stemming of As mobilized from disposed filter-sand material now re-adsorbed in a slightly tighter coordination onto soils (arrows in Figure 4C).

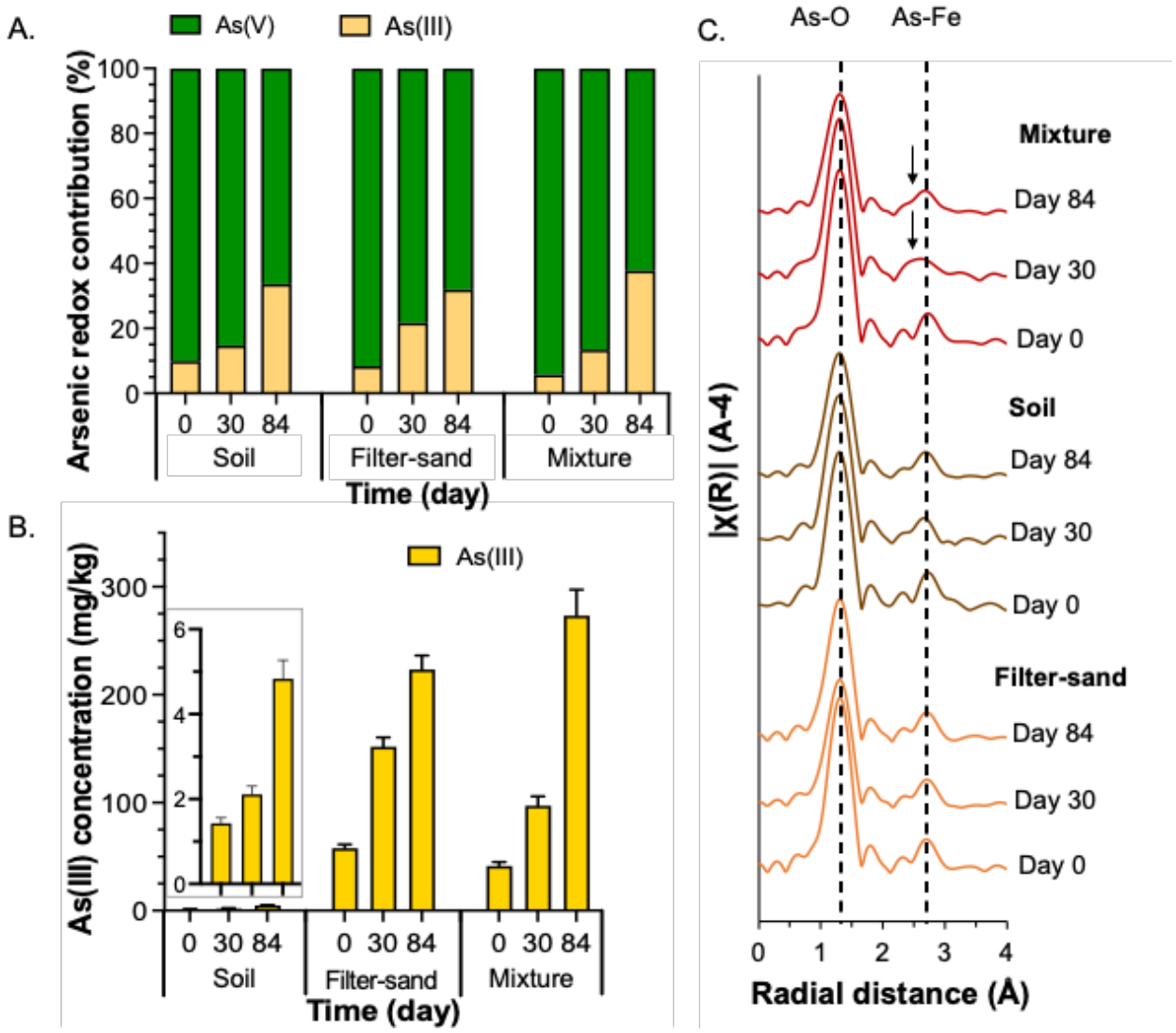

Figure 4. Changes of As redox contribution obtained by LC fitting of XANES data (A) calculated solid phase As(III) concentration combing XANES data and extraction data (B) and As K-edge EXAFS Fourier transform magnitude (C) over time in 3 different microcosms (soil, filter-sand, and the mixture of filter-sand and soil). Arsenic EXAFS *k*3 graphs of samples are shown in the supplement Figure S8.

Dynamics of colloidal Fe and As in the microcosms.

In our microcosms, we observed colloids that regularly remained suspended near the top of the solution. This led us to investigate changes in Fe and As contents in the colloidal fraction, as they can also be potentially mobilized and are reactive. We investigated the changes of Fe and As in the colloidal fraction at 3-time points (days 0, 30, and 100) by single particle ICP-MS (spICP-MS). Our previous work already showed a strong correlation between colloidal Fe and As but not with Al, suggesting that colloidal Fe is the main carrier of As instead of Al(Mansor et al., 2021).

Consistent with our expectation, the results indicated that the filter-sand material was the main source of colloidal Fe and As at day 0, with mass concentrations of 115 mg/L Fe and 240 μg/L As, respectively (Figure 5). These concentrations are much higher than dissolved Fe and As measured in the microcosms. In comparison, lower amounts of colloidal Fe and As were detectable in soil microcosms. The mixture of filter-sand and soil had intermediate amounts of colloidal Fe and As, in-between the unmixed filter-sand and soil microcosms. The colloidal Fe/As ratios were elevated by a factor of 5 to 141 compared to the microwave digestion-extractable fraction. This is likely due to the presence of small (but detectable) Fe-rich particles with As contents below the detection limit of spICP-MS (0.81 fg As/particle; Table S5), thus causing elevated colloidal Fe/As ratios. Over 100 days of incubation, we observed colloidal Fe and As decreased over time. The most pronounced decrease was observed in the mixture microcosms, in which over 90% of the colloidal mass was removed by the end (Figure 5).

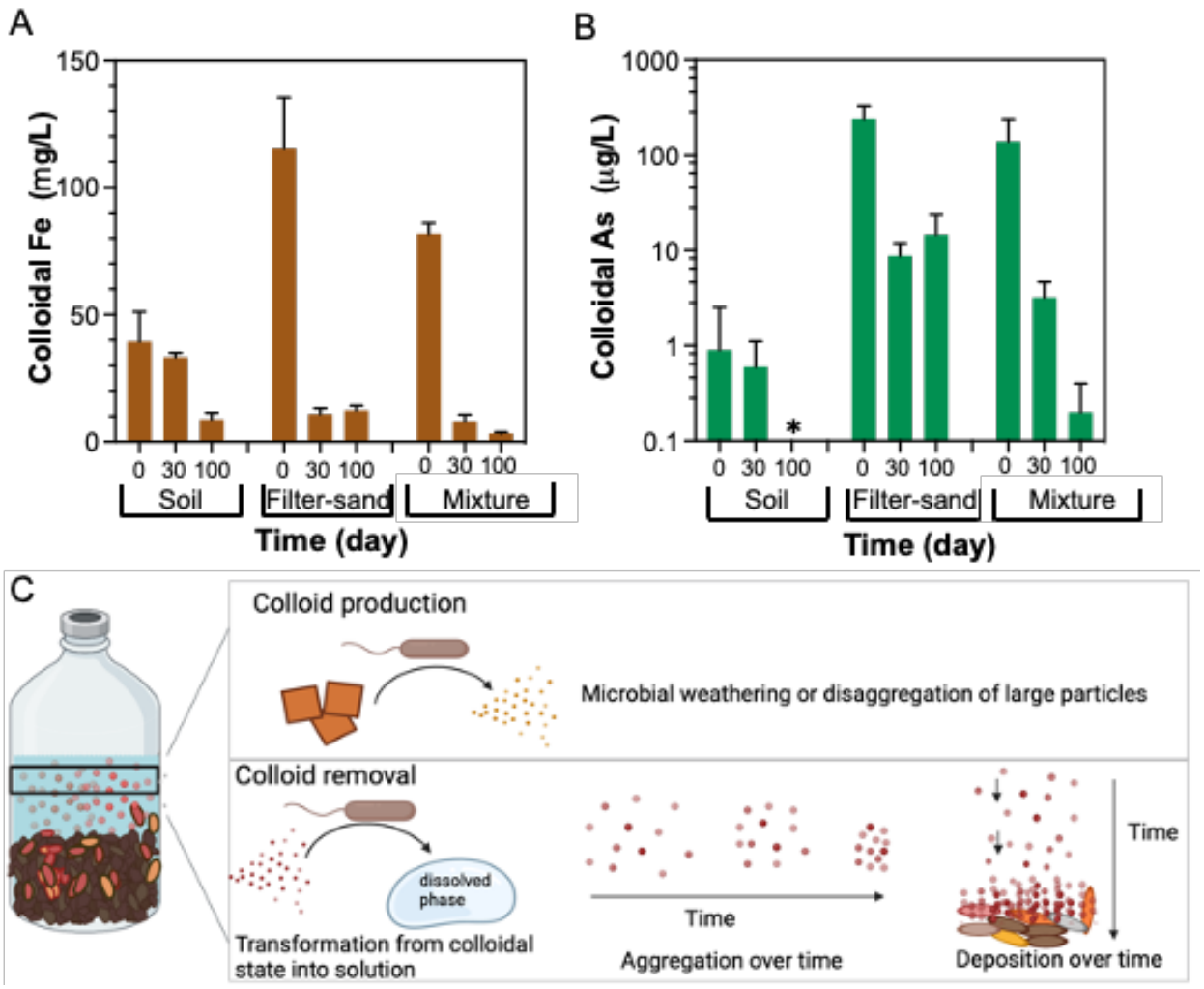

Figure 5. Changes in colloidal mass concentration of Fe and As in microcosms (A and B, respectively) containing either soil, disposed filter-sand or the mixture of filter-sand and soil over time. All samples were analyzed in triplicate and error bars indicate standard deviation. (*) No colloidal As detected in soil microcosms at day 100. Schematic conceptualization of colloid production and removal in the microcosms is shown in figure C.

Sand-soil interactions promote Fe and As reduction, leading to As mobilization.

Our results indicated that open disposal of filter-sand to soils and mixing between the two can promote microbial reduction and mobilization of As-bearing Fe(III) (oxyhydr)oxides. We propose

three non-exclusive mechanisms that can explain this observation. First, sand materials provide Fe(III) minerals that are more reactive (e.g., ferrihydrite) compared to those found in soils (e.g., goethite, hematite). Microbial reduction rates of ferrihydrite are generally up to 2 orders of magnitude faster than for goethite and hematite that were in the soil samples(Cutting et al., 2009; Kappler et al., 2021). Second, soil-associated organic carbon is likely to be more reactive than organic carbon associated with sand materials. During the flood season (June to October), massive amounts of organic-rich fluvial sediment are deposited in floodplain soils(Connolly et al., 2022; Smedley and Kinniburgh, 2002). The soil organic carbon in the Red River delta was previously identified to be derived predominantly from C_3/C_4 plant(Eiche et al., 2017). The water extractable fraction of this organic matter was shown to trigger microbial reduction of As-bearing Fe(III) (oxyhydr)oxides in the same sediments(Glodowska et al., 2020). Last but not least, microbial input from the soil to the filter-sand can promote the activities of iron(III)- and arsenic(V)-reducing bacteria in the mixture of filter-sand and soil. Iron-reducing bacteria such as *Shewanella* and *Geobacter* are common bacterial groups that are responsible for microbial reductive dissolution of As-bearing Fe(III) (oxyhydr)oxides in flooded soil(Corsini et al., 2011; Huang, 2014). Additionally, arsenate reducers are phylogenetically diverse and frequently present in paddy soils. They can directly reduce As(V) to toxic As(III) via dissimilation (ArrAB gene) or detoxification (*ars* gene) mechanisms(Huang, 2014; Vaxevanidou et al., 2015, 2012; Zhu et al., 2017).

Colloidal Fe and As were observed in our system, suggesting that As mobilization in the form of colloids could be substantial. Colloids can form in the environment due to seasonal water table changes and physical perturbation such as caused by heavy precipitation(Kretzschmar et al., 1999; Ma et al., 2018; Zhao et al., 2017). The production and removal mechanisms of colloids in the microcosms are schematized in Figure 5C. In our microcosms, colloids are produced by partial dissolution or disaggregation (weathering) of larger particles(Hochella Jr et al., 2019). Conversely,

colloids can be removed by i) complete dissolution of colloidal particles and ii) aggregation or deposition over time to form larger particles(Kretzschmar et al., 1999; Noël et al., 2020). Despite high concentrations of colloids at the initial stages of our experiments, we observed a strong decrease in colloidal As and Fe over time. This indicates a lower risk of colloidal As mobilization over time, and the removal of colloids is faster than their production in our experiments.

There are two possible reasons for this observation. First, since colloids are highly reactive and bioavailable, anaerobic bacteria might prefer Fe(III) and As(V) in the colloidal fraction to obtain energy for growth. Indeed, the reduction rate of Fe(III)-reducers such as *Geobacter* and *Shewanella* species are faster when supplied with small-sized Fe(III) (oxyhydr)oxides(Mansor and Xu, 2020). Since the amount of colloidal Fe and As made up <1.2 % of the total Fe and As extractable by aqua regia, a significant amount of colloids can be reduced without impacting the mass balance of the system.

Alternatively, since our microcosms were incubated standing with brief shaking only before sampling, there was ample time over the 100 days incubation period for aggregation and deposition of colloids to proceed. The stability of Fe colloids can be considered in terms of the C/Fe ratio of the systems. At low organic C/Fe ratios, as found in our experiments (C/Fe < 0.2), colloidal Fe is not stabilized by organic matter(Liao et al., 2017). Therefore, the colloids were more susceptible to forming larger aggregates(Amstaetter et al., 2012; Liao et al., 2017). This was followed by the deposition of the colloids by gravitational sedimentation over time, with larger aggregates leading to faster deposition(Liao et al., 2017).

5. ENVIRONMENTAL IMPLICATIONS

Our results indicated that a combined total of 116-390 μg/L of aqueous and colloidal As (0.3-4% of total As) was released from the solid phase. The remaining 96.0-99.7% of As was retained in

the solid phases. In comparison, a recent estimate suggests that 100% of the As from open disposal will be mobilized to either soils or water over 100 years(Genuchten et al., 2022) . The comparison between our experiments and this model estimation is not direct, but our results would at least suggest that As can be retained in the original solid phases over a period of a few months. Therefore, we anticipate different implications of As remobilization from filter-sand materials. First, short-distance transport (centimeters to meters) can lead to As being retained primarily in the surrounding soils. This is not an immediate concern unless the soil is then used for agricultural purposes, in which case this can lead to increased As contents in consumable plants. Second, frequent flooding and anoxic conditions can lead to enhanced long-distance transport (e.g., kilometers) of As in the form of colloids and aqueous phases, entering water sources such as aquifers and rivers. This is especially bad if As is released into groundwater aquifers, wells or rivers that are used for drinking water consumption and which were previously tested to have low As concentrations below the drinking water threshold. Thus, continuous testing is recommended for areas that utilize the open disposal method. The ultimate fate of remobilized As will need to be constrained in the context of flooding events(Connolly et al., 2022) and the heterogenous distribution of As in soils(Fakhreddine et al., 2021), and these will have varying influence from site-to-site.

Redox fluctuations are particularly important in the field due to changes in precipitation frequency throughout the year. Redox fluctuations can influence the crystallinity of Fe(III) (oxyhydr)oxides(Thompson et al., 2006). Ferrihydrite – the main host of As – can be transformed into more crystalline phases such as goethite or hematite as a result of redox fluctuations(Kocar and Fendorf, 2009). Additionally, redox fluctuations can promote organic carbon degradation in the aerobic zones near the surface, thus limiting the availability of organic carbon for anaerobic metabolisms at depth(Stuckey et al., 2016). Incubation under cycled redox conditions is required

in future experiments to understand changes in Fe mineralogy, organic carbon availability, and how these affect the release of colloidal and aqueous As.

ASSOCIATED CONTENT

Supporting information

Details description of microwave digestion, XAS and spICP-MS analysis, additional figures of extractable Fe(II)/Fe(total) by 6M HCl in all microcosms, fitting results of Moessbauer spectroscopy, As XANES, EXAFS, shell-by-shell fitting, and particle number concentration of Fe and As by spICP-MS.

AUTHOR INFORMATION

Corresponding author

Muammar Mansor - Geomicrobiology, Department of Geosciences, University of Tuebingen, 72076 Tuebingen, Germany; orcid.org/0000-0001-7830-650X

Phone: +49 7071 - 29 78999; Email: muammar.muammar-bin-mansor@uni-tuebingen.de

Authors

Anh Van Le - Geomicrobiology, Department of Geosciences, University of Tuebingen, 72076 Tuebingen, Germany

E. Marie Muehe - Plant Biogeochemistry, Department of Environmental Microbiology, Helmholtz Centre for Environmental Research - UFZ, 04318 Leipzig, Germany; and Plant Biogeochemistry, Department of Geosciences, University of Tuebingen, 72076 Tuebingen, Germany

Sören Drabesch - Geomicrobiology, Department of Geosciences, University of Tuebingen, 72076 Tuebingen, Germany

Juan Lezama Pacheco - Department of Environmental Earth System Science, Stanford University, Stanford, 94305 California, United States

Timm Bayer - Geomicrobiology, Department of Geosciences, University of Tuebingen, 72076 Tuebingen, Germany

Prachi Joshi - Geomicrobiology, Department of Geosciences, University of Tuebingen, 72076 Tuebingen, Germany; orcid.org/0000-0001-5954-0309

Andreas Kappler - Geomicrobiology Department of Geosciences, University of Tuebingen, 72076 Tuebingen, Germany; and Cluster of Excellence: EXC 2124: Controlling Microbes to Fight Infection, University of Tuebingen, 72076 Tuebingen, Germany; orcid.org/0000-0002-3558-9500

AUTHOR CONTRIBUTIONS

AK obtained funding and conceptualized the study. Sampling campaigns, lab work, and manuscript writing were done by A.V.L with the support and feedback of M.M and A.K. Sample preparation, measurement, and data analysis for XAS were done by J.L.P, E.M.M and S.D. The Moessbauer spectra were collected by and analyzed by T.B. and P.J. The manuscript was revised by all co-authors.

Notes

The authors declare no competing financial interest.

ACKNOWLEDGEMENTS

This work was funded by the German Research Foundation (DFG, KA1736/41-1). We thank M. Latimer for beamline support (proposal number 5587). Use of the Stanford Synchrotron Radiation Lightsource, SLAC National Accelerator Laboratory, is supported by the U.S. Department of Energy, Office of Science, Office of Basic Energy Sciences under Contract No. DE-AC02-

76SF00515. The SSRL Structural Molecular Biology Program is supported by the DOE Office of Biological and Environmental Research, and by the National Institutes of Health, National Institute of General Medical Sciences (including P41GM103393). The contents of this publication are solely the responsibility of the authors and do not necessarily represent the official views of NIGMS or NIH. AVL acknowledges the feedbacks from S.J.Hug for the manuscript and the help of P.Tutiyasarn and T.Schlereth for sampling and experiment setup. AK acknowledges infrastructural support by the DFG under Germany's Excellence Strategy, cluster of Excellence EXC2124, project ID 390838134. Graphical abstract created with BioRender.com.

REFERENCES

Amstaetter, K., Borch, T., Kappler, A., 2012. Influence of humic acid imposed changes of ferrihydrite aggregation on microbial Fe(III) reduction. Geochim. Cosmochim. Acta 85, 326–341. https://doi.org/10.1016/j.gca.2012.02.003

Bauer, M., Blodau, C., 2009. Arsenic distribution in the dissolved, colloidal and particulate size fraction of experimental solutions rich in dissolved organic matter and ferric iron. Geochim. Cosmochim. Acta 73, 529–542. https://doi.org/10.1016/j.gca.2008.10.030

Berg, M., Stengel, C., Trang, P.T.K., Hung Viet, P., Sampson, M.L., Leng, M., Samreth, S., Fredericks, D., 2007. Magnitude of arsenic pollution in the Mekong and Red River Deltas - Cambodia and Vietnam. Sci. Total Environ. 372, 413–425. https://doi.org/10.1016/j.scitotenv.2006.09.010

Bore, E.K., Apostel, C., Halicki, S., Kuzyakov, Y., Dippold, M.A., 2017. Soil microorganisms can overcome respiration inhibition by coupling intra-and extracellular metabolism: 13C metabolic tracing reveals the mechanisms. ISME J. 11, 1423–1433. https://doi.org/10.1038/ismej.2017.3

514 Cancès, B., Juillot, F., Morin, G., Laperche, V., Alvarez, L., Proux, O., Hazemann, J.-L., Brown,
515 G.E., Calas, G., 2005. XAS evidence of As (V) association with iron oxyhydroxides in a
516 contaminated soil at a former arsenical pesticide processing plant. Environ. Sci. Technol. 39,
517 9398–9405.
518 Catalano, J.G., Park, C., Fenter, P., Zhang, Z., 2008. Simultaneous inner-and outer-sphere
519 arsenate adsorption on corundum and hematite. Geochim. Cosmochim. Acta 72, 1986–2004.
520 Clancy, T.M., Hayes, K.F., Raskin, L., 2013. Arsenic waste management: A critical review of
521 testing and disposal of arsenic-bearing solid wastes generated during arsenic removal from
522 drinking water. Environ. Sci. Technol. 47, 10799–10812. https://doi.org/10.1021/es401749b
523 Connolly, C.T., Stahl, M.O., DeYoung, B.A., Bostick, B.C., 2022. Surface Flooding as a Key
524 Driver of Groundwater Arsenic Contamination in Southeast Asia. Environ. Sci. Technol. 56,
525 928–937. https://doi.org/10.1021/acs.est.1c05955
526 Corsini, A., Cavalca, L., Zaccheo, P., Crippa, L., Andreoni, V., 2011. Influence of
527 microorganisms on arsenic mobilization and speciation in a submerged contaminated soil:
528 Effects of citrate. Appl. Soil Ecol. 49, 99–106. https://doi.org/10.1016/j.apsoil.2011.06.010
529 Cutting, R.S., Coker, V.S., Fellowes, J.W., Lloyd, J.R., Vaughan, D.J., 2009. Mineralogical and
530 morphological constraints on the reduction of Fe (III) minerals by Geobacter sulfurreducens.
531 Geochim. Cosmochim. Acta 73, 4004–4022.
532 Dixit, S., Hering, J.G., 2003. Comparison of arsenic(V) and arsenic(III) sorption onto iron oxide
533 minerals: Implications for arsenic mobility. Environ. Sci. Technol. 37, 4182–4189.
534 https://doi.org/10.1021/es030309t
535 Eiche, E., Berg, M., Hönig, S.M., Neumann, T., Lan, V.M., Pham, T.K.T., Pham, H.V., 2017.
536 Origin and availability of organic matter leading to arsenic mobilisation in aquifers of the
537 Red River Delta, Vietnam. Appl. Geochemistry 77, 184–193.

https://doi.org/10.1016/j.apgeochem.2016.01.006

Fakhreddine, S., Prommer, H., Scanlon, B.R., Ying, S.C., Nicot, J.P., 2021. Mobilization of arsenic and other naturally occurring contaminants during managed aquifer recharge: A critical review. Environ. Sci. Technol. 55, 2208–2223. https://doi.org/10.1021/acs.est.0c07492

Fan, L., Zhao, F., Liu, J., Frost, R.L., 2018. The As behavior of natural arsenical-containing colloidal ferric oxyhydroxide reacted with sulfate reducing bacteria. Chem. Eng. J. 332, 183–191. https://doi.org/10.1016/j.cej.2017.09.078

Fendorf, S., Eick, M.J., Grossl, P., Sparks, D.L., 1997. Arsenate and chromate retention mechanisms on goethite. 1. Surface structure. Environ. Sci. Technol. 31, 315–320. https://doi.org/10.1021/es950653t

General Statistics Office of Vietnam, 2011. The Vietnam Population and Housing Census 2009—Age-sex structure and marital status of the population in Vietnam.

Genuchten, C.M. Van, Etmannski, T.R., Jessen, S., Breunig, H.M., 2022. LCA of Disposal Practices for Arsenic-Bearing Iron Oxides Reveals the. https://doi.org/10.1021/acs.est.2c05417

Ghosh, A., Mukiibi, M., Ela, W., 2004. TCLP underestimates leaching of arsenic from solid residuals under landfill conditions. Environ. Sci. Technol. 38, 4677–4682. https://doi.org/10.1021/es030707w

Glodowska, M., Stopelli, E., Schneider, M., Lightfoot, A., Rathi, B., Straub, D., Patzner, M., Duyen, V.T., Berg, M., Kleindienst, S., Kappler, A., 2020. Role of in Situ Natural Organic Matter in Mobilizing As during Microbial Reduction of FeIII-Mineral-Bearing Aquifer Sediments from Hanoi (Vietnam). Environ. Sci. Technol. 54, 4149–4159. https://doi.org/10.1021/acs.est.9b07183

562 Gomez-Gonzalez, M.A., Bolea, E., O'Day, P.A., Garcia-Guinea, J., Garrido, F., Laborda, F.,
563 2016. Combining single-particle inductively coupled plasma mass spectrometry and X-ray
564 absorption spectroscopy to evaluate the release of colloidal arsenic from environmental
565 samples. Anal. Bioanal. Chem. 408, 5125–5135.
566 Ha, N.T.H., Ha, N.T., Nga, T.T.H., Minh, N.N., Anh, B.T.K., Hang, N.T.A., Duc, N.A., Nhuan,
567 M.T., Kim, K.W., 2019. Uptake of arsenic and heavy metals by native plants growing near
568 Nui Phao multi-metal mine, northern Vietnam. Appl. Geochemistry 108.
569 https://doi.org/10.1016/j.apgeochem.2019.104368
570 Hassellov, M., von der Kammer, F., 2008. Iron oxides as geochemical nanovectors for metal
571 transport in soil-river systems. Elements 4, 401–406.
572 Hoang, A.T.P., Prinpreecha, N., Kim, K.W., 2021. Influence of mining activities on arsenic
573 concentration in rice in asia: A review. Minerals 11, 1–14.
574 https://doi.org/10.3390/min11050472
575 Hochella Jr, M.F., Mogk, D.W., Ranville, J., Allen, I.C., Luther, G.W., Marr, L.C., McGrail,
576 B.P., Murayama, M., Qafoku, N.P., Rosso, K.M., 2019. Natural, incidental, and engineered
577 nanomaterials and their impacts on the Earth system. Science (80-.). 363, eaau8299.
578 Huang, J.H., 2014. Impact of microorganisms on arsenic biogeochemistry: A review. Water. Air.
579 Soil Pollut. 225. https://doi.org/10.1007/s11270-013-1848-y
580 Ippolito, J.A., Barbarick, K.A., Elliott, H.A., 2011. Drinking Water Treatment Residuals : A
581 Review of Recent Uses 2, 1–12. https://doi.org/10.2134/jeq2010.0242
582 Islam, M.S., Al Mamun, M.A., Islam, M.N., 2011. Leachability Of Arsenic From Wastes Of
583 Arsenic Removal Units Using Modified Toxicity Characteristic Leaching Procedure. J. Life
584 Earth Sci. 6, 19–26. https://doi.org/10.3329/jles.v6i0.9716
585 Kappler, A., Bryce, C., Mansor, M., Lueder, U., Byrne, J.M., Swanner, E.D., 2021. An evolving

view on biogeochemical cycling of iron. Nat. Rev. Microbiol. 19, 360–374. https://doi.org/10.1038/s41579-020-00502-7

Kocar, B.D., Fendorf, S., 2009. Thermodynamic constraints on reductive reactions influencing the biogeochemistry of arsenic in soils and sediments. Environ. Sci. Technol. 43, 4871–4877. https://doi.org/10.1021/es8035384

Koley, S., 2022. Future perspectives and mitigation strategies towards groundwater arsenic contamination in West Bengal, India. Environ. Qual. Manag. 31, 75–97. https://doi.org/10.1002/tqem.21784

Kretzschmar, R., Borkovec, M., Grolimund, D., Elimelech, M., 1999. Mobile Subsurface Colloids and Their Role in Contaminant Transport. Adv. Agron. 66, 121–193. https://doi.org/10.1016/S0065-2113(08)60427-7

Lagarec, K., Rancourt, D.G., 1997. Extended Voigt-based analytic lineshape method for determining N-dimensional correlated hyperfine parameter distributions in Mössbauer spectroscopy. Nucl. Instruments Methods Phys. Res. Sect. B Beam Interact. with Mater. Atoms 129, 266–280.

Liao, P., Li, W., Jiang, Y., Wu, J., Yuan, S., Fortner, J.D., Giammar, D.E., 2017. Formation, aggregation, and deposition dynamics of nom-iron colloids at anoxic-oxic interfaces. Environ. Sci. Technol. 51, 12235–12245. https://doi.org/10.1021/acs.est.7b02356

Ma, J., Guo, H., Weng, L., Li, Y., Lei, M., Chen, Y., 2018. Distinct effect of humic acid on ferrihydrite colloid-facilitated transport of arsenic in saturated media at different pH. Chemosphere 212, 794–801. https://doi.org/10.1016/j.chemosphere.2018.08.131

Manning, B.A., Fendorf, S.E., Goldberg, S., 1998. Surface structures and stability of arsenic(III) on goethite: Spectroscopic evidence for inner-sphere complexes. Environ. Sci. Technol. 32, 2383–2388. https://doi.org/10.1021/es9802201

610 Mansor, M., Drabesch, S., Bayer, T., Van Le, A., Chauhan, A., Schmidtmann, J., Peiffer, S.,
611 Kappler, A., 2021. Application of Single-Particle ICP-MS to Determine the Mass
612 Distribution and Number Concentrations of Environmental Nanoparticles and Colloids.
613 Environ. Sci. Technol. Lett. https://doi.org/10.1021/acs.estlett.1c00314
614 Mansor, M., Xu, J., 2020. Benefits at the nanoscale: a review of nanoparticle-enabled processes
615 favouring microbial growth and functionality. Environ. Microbiol. 22, 3633–3649.
616 https://doi.org/10.1111/1462-2920.15174
617 Montalvo, D., Vanderschueren, R., Fritzsche, A., Meckenstock, R.U., Smolders, E., 2018.
618 Efficient removal of arsenate from oxic contaminated water by colloidal humic acid-coated
619 goethite: Batch and column experiments. J. Clean. Prod. 189, 510–518.
620 https://doi.org/10.1016/j.jclepro.2018.04.055
621 Muehe, E.M., Morin, G., Scheer, L., Le Pape, P., Esteve, I., Daus, B., Kappler, A., 2016.
622 Arsenic(V) Incorporation in Vivianite during Microbial Reduction of Arsenic(V)-Bearing
623 Biogenic Fe(III) (Oxyhydr)oxides. Environ. Sci. Technol. 50, 2281–2291.
624 https://doi.org/10.1021/acs.est.5b04625
625 Muehe, E.M., Obst, M., Hitchcock, A., Tyliszczak, T., Behrens, S., Schröder, C., Byrne, J.M.,
626 Michel, F.M., Krämer, U., Kappler, A., 2013. Fate of Cd during microbial Fe (III) mineral
627 reduction by a novel and Cd-tolerant Geobacter species. Environ. Sci. Technol. 47, 14099–
628 14109.
629 Nitzsche, K.S., Lan, V.M., Trang, P.T.K., Viet, P.H., Berg, M., Voegelin, A., Planer-Friedrich,
630 B., Zahoransky, J., Müller, S.K., Byrne, J.M., Schröder, C., Behrens, S., Kappler, A., 2015.
631 Arsenic removal from drinking water by a household sand filter in Vietnam - Effect of filter
632 usage practices on arsenic removal efficiency and microbiological water quality. Sci. Total
633 Environ. 502, 526–536. https://doi.org/10.1016/j.scitotenv.2014.09.055

Noël, V., Kumar, N., Boye, K., Barragan, L., Lezama-Pacheco, J.S., Chu, R., Tolic, N., Brown, G.E., Bargar, J.R., 2020. FeS colloids–formation and mobilization pathways in natural waters. Environ. Sci. Nano 7, 2102–2116.

Notini, L., Latta, D.E., Neumann, A., Pearce, C.I., Sassi, M., N'Diaye, A.T., Rosso, K.M., Scherer, M.M., 2018. The role of defects in Fe (II)–goethite electron transfer. Environ. Sci. Technol. 52, 2751–2759.

O'Day, P.A., Rivera Jr, N., Root, R., Carroll, S.A., 2004. X-ray absorption spectroscopic study of Fe reference compounds for the analysis of natural sediments. Am. Mineral. 89, 572–585.

Ona-Nguema, G., Morin, G., Juillot, F., Calas, G., Brown, G.E., 2005. EXAFS analysis of arsenite adsorption onto two-line ferrihydrite, hematite, goethite, and lepidocrocite. Environ. Sci. Technol. 39, 9147–9155. https://doi.org/10.1021/es050889p

Oremland, R.S., Stolz, J.F., 2003. The ecology of arsenic. Science (80-.). 300, 939–944. https://doi.org/10.1126/science.1081903

Raiswell, R., Canfield, D.E., Berner, R.A., 1994. A comparison of iron extraction methods for the determination of degree of pyritisation and the recognition of iron-limited pyrite formation. Chem. Geol. 111, 101–110.

Ravel, B., Newville, M., 2005. ATHENA, ARTEMIS, HEPHAESTUS: data analysis for X-ray absorption spectroscopy using IFEFFIT. J. Synchrotron Radiat. 12, 537–541.

Schaedler, F., Kappler, A., Schmidt, C., 2018. A revised iron extraction protocol for environmental samples rich in nitrite and carbonate. Geomicrobiol. J. 35, 23–30.

Sherman, D.M., Randall, S.R., 2003. Surface complexation of arsenic(V) to iron(III) (hydr)oxides: Structural mechanism from ab initio molecular geometries and EXAFS spectroscopy. Geochim. Cosmochim. Acta 67, 4223–4230. https://doi.org/10.1016/S0016-7037(03)00237-0

Smedley, P.L., Kinniburgh, D.G., 2002. A review of the source, behaviour and distribution of arsenic in natural waters. Appl. Geochemistry 17, 517–568. https://doi.org/10.1016/S0883-2927(02)00018-5

Stookey, L.L., 1970. Ferrozine---a new spectrophotometric reagent for iron. Anal. Chem. 42, 779–781.

Stuckey, J.W., Schaefer, M. V., Kocar, B.D., Benner, S.G., Fendorf, S., 2016. Arsenic release metabolically limited to permanently water-saturated soil in Mekong Delta. Nat. Geosci. 9, 70–76. https://doi.org/10.1038/ngeo2589

Sullivan, C., Tyrer, M., Cheeseman, C.R., Graham, N.J.D., 2010. Disposal of water treatment wastes containing arsenic - A review. Sci. Total Environ. 408, 1770–1778. https://doi.org/10.1016/j.scitotenv.2010.01.010

Thompson, A., Chadwick, O.A., Boman, S., Chorover, J., 2006. Colloid mobilization during soil iron redox oscillations. Environ. Sci. Technol. 40, 5743–5749. https://doi.org/10.1021/es061203b

Turner, T., Wheeler, R., Stone, A., Oliver, I., 2019. Potential Alternative Reuse Pathways for Water Treatment Residuals: Remaining Barriers and Questions—a Review. Water. Air. Soil Pollut. 230. https://doi.org/10.1007/s11270-019-4272-0

Van Le, A., Straub, D., Planer-Friedrich, B., Hug, S.J., Kleindienst, S., Kappler, A., 2022. Microbial communities contribute to the elimination of As, Fe, Mn, and NH4+ from groundwater in household sand filters. Sci. Total Environ. 838, 156496. https://doi.org/10.1016/j.scitotenv.2022.156496

Vaxevanidou, K., Christou, C., Kremmydas, G.F., Georgakopoulos, D.G., Papassiopi, N., 2015. Role of indigenous arsenate and IRON(III) respiring microorganisms in controlling the mobilization of arsenic in a contaminated soil sample. Bull. Environ. Contam. Toxicol. 94,

282–288. https://doi.org/10.1007/s00128-015-1458-z

Vaxevanidou, K., Giannikou, S., Papassiopi, N., 2012. Microbial arsenic reduction in polluted and unpolluted soils from Attica, Greece. J. Hazard. Mater. 241–242, 307–315. https://doi.org/10.1016/j.jhazmat.2012.09.048

Viollier, E., Inglett, P.W., Hunter, K., Roychoudhury, A.N., Van Cappellen, P., 2000. The ferrozine method revisited: Fe (II)/Fe (III) determination in natural waters. Appl. geochemistry 15, 785–790.

Voegelin, Andreas; Kaegi, Ralf; Berg, Michael; Nitzsche, Katja Sonja; Kappler, Andreas; Lan, Vi Mai; Trang, Pham Thi Kim; Göttlicher, Jörg; Steininger, R., 2014. Solid-phase characterisation of an effective household sand filter for As, Fe and Mn removal from groundwater in Vietnam. Environ. Chem. 11, 566–578. https://doi.org/10.1071/EN14011

Webb, S.M., 2005. SIXpack: a graphical user interface for XAS analysis using IFEFFIT. Phys. Scr. 2005, 1011.

Winkel, L.H.E., Trang, P.T.K., Lan, V.M., Stengel, C., Amini, M., Ha, N.T., Viet, P.H., Berg, M., 2011. Arsenic pollution of groundwater in Vietnam exacerbated by deep aquifer exploitation for more than a century. Proc. Natl. Acad. Sci. U. S. A. 108, 1246–1251. https://doi.org/10.1073/pnas.1011915108

Yao, Y., Mi, N., He, C., Yin, L., Zhou, D., Zhang, Y., Sun, H., Yang, S., Li, S., He, H., 2020. Transport of arsenic loaded by ferric humate colloid in saturated porous media. Chemosphere 240. https://doi.org/10.1016/j.chemosphere.2019.124987

Zhao, J., Chen, S., Hu, R., Li, Y., 2017. Aggregate stability and size distribution of red soils under different land uses integrally regulated by soil organic matter, and iron and aluminum oxides. Soil Tillage Res. 167, 73–79. https://doi.org/10.1016/j.still.2016.11.007

Zhu, Y.G., Xue, X.M., Kappler, A., Rosen, B.P., Meharg, A.A., 2017. Linking Genes to

706 Microbial Biogeochemical Cycling: Lessons from Arsenic. Environ. Sci. Technol. 51, 7326–
707 7339. https://doi.org/10.1021/acs.est.7b00689
708